

Performance Analysis of NR Sidelink and Wi-Fi Coexistence Networks in Unlicensed Spectrum

Zhuangzhuang Yan, Xinyu Gu, *Member, IEEE*, Zhenyu Liu, *Member, IEEE*,

Abstract—With the rapid development of various internet of things (IoT) applications, including industrial IoT (IIoT) and visual IoT (VIoT), the demand for direct device-to-device communication to support high data rates continues to grow. To address this demand, 5G-Advanced has introduced sidelink communication over the unlicensed spectrum (SL-U) as a method to increase data rates. However, the primary challenge of SL-U in the unlicensed spectrum is ensuring fair coexistence with other incumbent systems, such as Wi-Fi. In this paper, we address the challenge by designing channel access mechanisms and power control strategies to mitigate interference and ensure fair coexistence. First, we propose a novel collaborative channel access (CCHA) mechanism that integrates channel access with resource allocation through collaborative interactions between base stations (BS) and SL-U users. This mechanism ensures fair coexistence with incumbent systems while improving resource utilization. Second, we mathematically model the joint channel access and power control problems, analyzing the trade-off between fairness and transmission rate to minimize interference and optimize performance in the coexistence system. Finally, we develop a collaborative subgoal-based hierarchical deep reinforcement learning (C-GHDRL) framework. This framework enables SL-U users to make globally optimal decisions by leveraging collaborative operations between the BS and SL-U users, effectively overcoming the limitations of traditional optimization methods in solving joint optimization problems with nonlinear constraints. Simulation results demonstrate that the proposed scheme significantly enhances the coexistence system's performance while ensuring fair coexistence between SL-U and Wi-Fi users.

Index Terms—SL-U, collaborative, hierarchical deep reinforcement learning, channel access, power control.

I. INTRODUCTION

WITH the advent of industry 5.0, driven by emerging applications such as predictive maintenance, hyper-customization in manufacturing, and collaborative robotics [1], the data rates of future Industrial Internet of Things (IIoT) systems are predicted to increase by 10 to 50 times compared to current networks [2]. Additionally, the Visual Internet of Things (VIoT) plays a crucial role in urban counter-terrorism, intelligent border security, and missing person searches by leveraging visual sensors to process and analyze real-time visual data streams intelligently [3]. Either the predictive maintenance within IIoT or the transmission of video streams in VIoT, sidelink (SL) communication with high data rates is required to deliver these services effectively. To address

the demand, the evolution of new radio (NR) sidelink [4], one of the initial projects approved by 5G-Advanced, offers a solution by utilizing sidelink over unlicensed spectrum (SL-U). SL-U is a novel wireless communication protocol that enables devices to communicate directly over unlicensed spectrum without relying on cellular networks or access points. It is highly suitable for short-distance wireless communication applications like the Internet of Things (IoT) [5].

While the introduction of SL-U can significantly enhance the data rate of wireless links, the primary challenge for SL-U is to ensure fair coexistence with other incumbent systems, such as Wi-Fi, in the unlicensed spectrum. The most critical of fair coexistence is the need for effective interference mitigation to ensure fair and efficient spectrum sharing [6–8]. To address the challenge, SL-U employs the listen-before-talk (LBT) channel access mechanism, which enables devices to perform a clear channel assessment (CCA) to sense channel availability prior to transmission [9]. However, the 3rd Generation Partnership Project (3GPP) standards specified that the minimum scheduling resource of physical sidelink shared channel (PSSCH) in the time domain is a slot [10]. Consequently, after completing the LBT process, SL-U users in the unlicensed spectrum are required to wait for the spectrum slot boundary (SSB) before initiating data transmission. This requirement may lead to channel access collisions and inefficient resource utilization. To address this issue, [11] proposed a method to reduce collisions by randomizing the starting position of the back-off countdown process within a slot. However, the approach is limited to SL-U-only networks and does not account for coexistence scenarios. [12] proposed a new CR-LBT (LBT With Collision Resolution) method of transmitting reserved signals, which greatly reduces collisions and enhances the fairness of channel resource sharing. However, the presence of reserved signals wastes channel resources.

In addition, selecting the appropriate transmission power for SL-U users after channel access is also essential for interference mitigation [13–15]. Considering inter-cell and inter-operator interference in both licensed and unlicensed spectrum, [16] proposed a joint optimization framework that integrates user association, power allocation, and dynamic spectrum sharing to maximize network throughput. [17] presented a joint power control and time allocation scheme for licensed and unlicensed spectrum in unmanned aerial vehicle (UAV)-assisted Internet of Vehicles (IoV) systems, optimizing power and time allocation to maximize overall system capacity.

Channel access and power control are two fundamental mechanisms for SL-U in the coexistence network, and they exhibit significant interdependence [11, 13, 18]. This interdepen-

Zhuangzhuang Yan and Xinyu Gu are with the School of Artificial Intelligence, Beijing University of Posts and Telecommunications, Beijing 100876, China (email: yanzz@bupt.edu.cn, guxinyu@bupt.edu.cn)

Zhenyu Liu is with the 5GIC and 6GIC, Institute for Communication Systems, University of Surrey, United Kingdom, Guildford, U.K.(email: zhenyu.liu@surrey.ac.uk)

dence becomes especially significant in unlicensed spectrum coexistence scenarios. For example, considering the coexistence of terrestrial cellular networks, Wi-Fi, and UAV-based base stations (UAV-BSs), [19] jointly optimized sub-channel allocation and power control of UAV users across the licensed and unlicensed spectrum to maximize the total uplink rate. [20] jointly optimized the time and power allocation during maximum channel occupation time (MCOT) to maximize the total throughput of both downlink and uplink in New Radio on unlicensed channel spectrum (NR-U) while ensuring fair coexistence with Wi-Fi. To this end, we jointly optimize channel access and power control to mitigate interference and enhance spectrum utilization. Various centralized algorithms based on combinatorial optimization [21], random geometry [22], and game theory [23] have been proposed for the joint optimization problem. However, the joint optimization of channel access and power control is often formulated as a combinatorial optimization problem with nonlinear constraints, which leads to the ineffectiveness of traditional optimization methods in most scenarios [13, 24].

The emergence of deep reinforcement learning (DRL) has introduced promising solutions to joint optimization problems with nonlinear constraints [25, 26]. In [27], a distributed DRL-based scheme was proposed, enabling D2D pairs to autonomously optimize channel selection and transmission power using only local information and outdated non-local information. [28] introduced a novel DRL-based framework for jointly optimizing power and block length allocation to minimize the worst-case decoding-error probability in the finite block length (FBL) regime for an ultra-reliable low-latency communication (URLLC) -based downlink V2X communication system. However, it is important to note that DRL-based approaches typically require all actions to operate on the same time scale when solving joint optimization problems, meaning that all actions must be decided simultaneously. This assumption may not be applicable in certain communication scenarios where actions occur at different timescales.

Therefore, hierarchical deep reinforcement learning (HDRL) is proposed to solve the problem [29–32]. By adopting a hierarchical learning framework, HDRL can achieve both global and local optimization, which is very suitable for the joint optimization of channel access and power control with different timescales. In [33], the authors optimized the CCA threshold and transmit power of the access point (AP) using the HDRL algorithm, improving network performance. However, [33] focuses solely on a scenario involving Wi-Fi users and does not address the coexistence challenges associated with the unlicensed spectrum. [34] proposed leveraging the HDRL algorithm to jointly optimize partial spectrum sensing and power allocation, enabling users to make intelligent decisions on spectrum selection and power allocation to maximize network throughput while minimizing mutual interference. Although each secondary user (SU) transmits information to the central server to train the HDRL neural network, the central server maintains a separate model for each user. As a result, each network is trained based solely on the local information available to the corresponding user, which may prevent the model from achieving a globally

optimal solution.

In summary, to address the issues of channel collisions and low resource utilization caused by time slot alignment for SL-U users, we propose a novel collaborative channel access (CCHA) mechanism. Additionally, we model the joint channel access and power control problem, analyzing strategies to enhance the overall performance of the coexistence system while balancing the trade-off between fairness and transmission rate. Finally, to overcome the challenges posed by the lack of an information-sharing mechanism between SL-U users in the unlicensed spectrum, which prevents models from making globally optimal decisions, and the inefficiency of traditional combinatorial optimization methods under nonlinear constraints, we developed a collaborative subgoal-based HDRL (C-GHDRL) algorithm framework. The framework achieves joint optimization of channel access and power control through collaborative interactions between the BS and SL-U users, thereby significantly improving the overall performance of the coexistence system. The main contributions of this paper are as follows:

- We propose a CCHA mechanism integrating channel access and resource allocation. In this mechanism, the BS allocates available resources to SL-U users within its coverage area based on channel sensing results. SL-U users assigned to these resources perform lightweight LBT before accessing the channel. This collaborative interaction between the BS and SL-U users not only ensures complete resource orthogonality but also increases the opportunities for channel access for SL-U users. Consequently, this mechanism enhances resource utilization and significantly improves coexistence system performance.
- For the SL-U and Wi-Fi coexistence system, we establish a mathematical joint model for the channel access and power control problems to analyze how to balance fairness and transmission rate under relevant constraints.
- We propose a C-GHDRL algorithm framework designed to jointly optimize channel access and power control for SL-U users in coexistence systems. In the framework, BS collects global information through interaction with SL-U users to train the C-GHDRL model and periodically distributes the trained model to all SL-U users. Each SL-U user applies this model autonomously to determine optimal channel access and transmission power. Through collaborative operations between the BS and SL-U users, the algorithm enables SL-U users to make globally optimal decisions while effectively addressing the joint optimization of channel access and power control under nonlinear constraints, thereby significantly improving the overall performance of coexistence systems.

The rest of this paper is organized as follows. Section II presents the system model as well as the problem formulation. In Section III, we elaborate on the proposed collaborative channel access mechanism. Joint optimization of channel access and power control based on the C-GHDRL algorithm is described in Section IV. Followed by performance evaluation and comparison in Section V. Finally, a conclusion is drawn

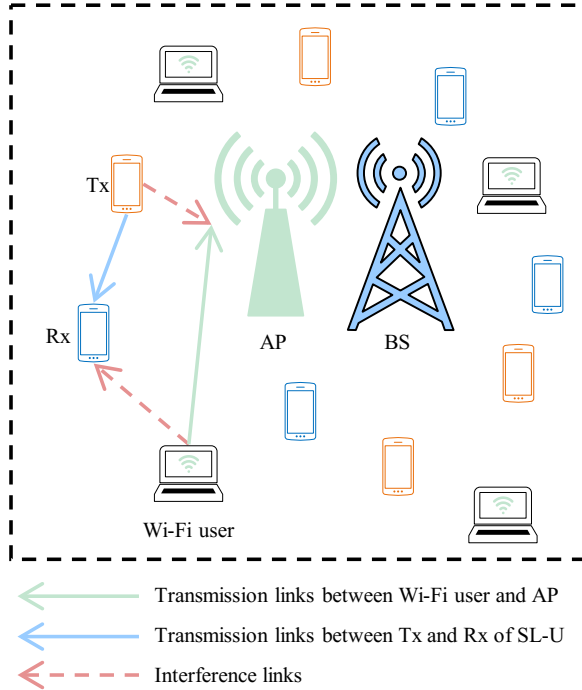


Fig. 1. Wi-Fi and SL-U coexistence scenario.

in Section VI.

II. SYSTEM MODEL AND PROBLEM FORMULATION

A. Network Model

Consider a communication scenario in which Wi-Fi and SL-U coexist in the unlicensed spectrum, as depicted in Fig. 1. This scenario includes a Wi-Fi AP, an SL-U BS, multiple Wi-Fi users, and multiple SL-U user pairs. Each SL-U user pair comprises a transmitter (Tx) and a receiver (Rx). The BS and AP are centrally located within the area, while Wi-Fi and SL-U users are randomly distributed. The distance between the Tx and Rx of each SL-U user pair is represented by a random variable, denoted as dis_{random} . Let $\mathcal{M} = \{1, 2, \dots, M\}$ denote the set of SL-U user pairs, and $\mathcal{N} = \{1, 2, \dots, N\}$ denote the set of Wi-Fi users. Define T_m and R_m as the transmitter and receiver of SL-U user pair $m \in \mathcal{M}$, respectively.

B. Channel Access Schemes over Unlicensed Spectrum

Both SL-U and Wi-Fi users compete for access to the unlicensed spectrum using contention-based access mechanisms. In the IEEE 802.11n protocol, Wi-Fi users used Carrier Sense Multiple Access with Collision Avoidance (CSMA/CA) to manage channel contention [35]. SL-U employed the LBT mechanism specified by 3GPP 37.213 [9]. In the following, we will provide a detailed description of these two channel access mechanisms.

- 1) **CSMA/CA:** As illustrated in Fig. 2, the CSMA/CA scheme incorporates a back-off mechanism to randomize the transmission start time of Wi-Fi users, thereby reducing the likelihood of collisions in the absence of a centralized coordination function. When a new data

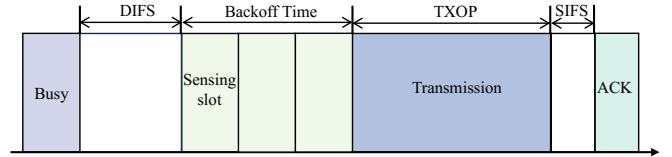


Fig. 2. CSMA/CA procedure of Wi-Fi.

packet arrives, Wi-Fi users perform carrier sensing to check the status of the wireless channel before initiating transmission. When the user senses that the wireless channel has been idle for distributed inter-frame space (DIFS), it will proceed to wait for a random time before sending data. The period of random waiting is called the random back-off time, and the operation of waiting for a random time is called the random back-off process. Once the back-off period concludes, the Wi-Fi user transmits their data during a transmission opportunity (TXOP). Upon successfully receiving the data, the AP waits for a short inter-frame space (SIFS) and sends an acknowledgment (ACK) to confirm the correct reception.

- 2) **LBT:** The LBT scheme adopts a similar back-off mechanism to that of the CSMA/CA protocol. Before initiating data transmission, an SL-U user performs CCA to sense whether the channel is busy or idle. If the channel remains idle for a specified period, denoted as T_d , the user initiates a back-off process, introducing a random time before attempting transmission. However, unlike in CSMA/CA, where users can transmit immediately after the back-off process concludes, SL-U users must wait for the next SSB before transmitting data. [9] defined two types of channel access processes for LBT:

- Type 1: Channel access procedure with random back-off of variable size contention window (CW). According to [9], the CW size is determined by the channel access priority p , as indicated in Table I.
- Type 2: No random backoff procedure is carried out, and only a predetermined period of channel sensing or no channel sensing is performed before accessing the channel.

C. Communication Model

For the Wi-Fi users path loss model, the free space loss model is used:

$$PL_w = 32.44 + 20 \times \log_{10} f_c + 20 \times \log_{10} (d_w), \quad (1)$$

where f_c and d_w are the center frequency in GHz and the distance between the Wi-Fi user and the AP in meters, respectively.

The SL-U users path loss model is based on the 3GPP standard and applies to line-of-sight (LOS) office scenarios[36]. The path loss model is as follows:

$$PL_s = 32.4 + 20 \times \log_{10} f_c + 17.3 \times \log_{10} (d_s), \quad (2)$$

where d_s is the distance between the transmitter and receiver of the SL-U user in meters. The corresponding shadow fading (SF) follows a log-normal distribution with a mean of 0 and a standard deviation of $\sigma_{SF} = 3$.

TABLE I
CHANNEL ACCESS PRIORITY CLASS (CAPC)

Channel Access Priority Class (p)	m_p	$CW_{min,p}$	$CW_{max,p}$	$T_{mcot,p}$	allowed CW_p sizes
1	2	3	7	2 ms	{3,7}
2	2	7	15	4 ms	{7,15}
3	3	15	1023	6 or 10 ms	{15,31,63,127,255,511,1023}
4	7	15	1023	6 or 10 ms	{15,31,63,127,255,511,1023}

Therefore, the signal-to-interference-to-noise ratio (SINR) of the SL-U pair m and the Wi-Fi user n in time slot t are respectively defined as:

$$\eta_{s,m}(t) = \frac{p_{s,m}^T(t) - PL_{s,m} - PL_{SF,m}}{p_{noise} + \sum_{n=0}^N k_{w,n}(t) p_{inter,w}^{R_{m,n}}(t)}, \quad (3)$$

$$\eta_{w,n}(t) = \frac{p_{w,n}^T(t) - PL_{w,n}}{p_{noise} + \sum_{m=0}^M k_{s,m}(t) p_{inter,s}^{AP,m}(t)}, \quad (4)$$

where $p_{s,m}^T(t)$ and $p_{w,n}^T(t)$ are the transmission power of SL-U user T_m and the Wi-Fi user n , respectively. The $PL_{s,m}$ and $PL_{SF,m}$ represent respectively the path loss and the shadow fading between the transmitter and receiver of the SL-U pair m . The $PL_{w,n}$ is the path loss of the Wi-Fi user n . The p_{noise} is additive Gaussian white noise (AWGN) power, $p_{inter,w}^{R_{m,n}}(t)$ represents the interference power received by SL-U R_m from Wi-Fi user n , $p_{inter,s}^{AP,m}(t)$ represents the interference power received by AP from SL-U T_m . If $k_{s,m}(t) = 1$ indicates that SL-U pair m accesses the channel during time slot t ; otherwise, $k_{s,m}(t) = 0$ indicates that SL-U pair m does not access the channel. If $k_{w,n}(t) = 1$ indicates that Wi-Fi user n accesses the channel during time slot t ; otherwise, $k_{w,n}(t) = 0$ indicates that Wi-Fi user n does not access the channel.

According to (3)(4), the transmission rate of the SL-U system and Wi-Fi system in slot t are respectively defined as:

$$R_s^C(t) = \sum_{m=0}^M k_{s,m}(t) B \log_2(1 + \eta_{s,m}(t)), \quad (5)$$

$$R_w^C(t) = \sum_{n=0}^N k_{w,n}(t) B \log_2(1 + \eta_{w,n}(t)), \quad (6)$$

where the B denotes channel bandwidth.

Therefore, the total transmission rate of the coexistence system in slot t is defined as:

$$R_{total}^C(t) = R_s^C(t) + R_w^C(t), \quad (7)$$

D. Fairness Model Analysis

Fairness measure is used in network engineering to determine whether users or applications are receiving a fair share of system resources. The formula for Jain's fairness index is as follows:

$$\mathcal{J}(x_1, x_2, \dots, x_n) = \frac{(\sum_{i=1}^n x_i)^2}{n \cdot \sum_{i=1}^n x_i^2} \in [\frac{1}{n}, 1], \quad (8)$$

where x_i is the throughput for the i th connection. n denotes the total number of users. According to the characteristics of Jain's fairness index, it is a continuous value from $1/n$ to 1. The index is 1 when all users receive the same allocation[37].

Although the SL-U system is authorized to transmit data in the unlicensed spectrum, it should not affect the performance of the Wi-Fi system. In this paper, we employ the Jain's fairness index, as described in (8), to ensure fairness in the coexistence system, which is expressed as follows:

$$\mathcal{J}\mathcal{F}^C = \frac{(R_s^C + R_w^C)^2}{2((R_s^C)^2 + (R_w^C)^2)}, \quad (9)$$

where R_s^C and R_w^C are the transmission rate attained by SL-U and Wi-Fi system during the simulation time, respectively.

E. Problem Formulation

In unlicensed spectrum coexistence systems, our objective is to maximize the transmission rate while maintaining fairness across the system. To comprehensively evaluate both the transmission rate and fairness between SL-U and Wi-Fi, we define the utility function as follows:

$$U(k, p) = \beta R_{total}^C + (1 - \beta) \mathcal{J}\mathcal{F}^C, \quad (10)$$

where β is a weighted factor to balance the transmission rate and the fairness.

We find that the maximizing utility function is closely related to channel access status k and transmission power p . Therefore, the mathematical formulation of the problem is given as follows:

$$P.F. : \arg \max_{\mathbf{k}, \mathbf{p}} U(\mathbf{k}, \mathbf{p}),$$

$$s.t. \quad C1 : p_{s,min}^T \leq p_{s,m}^T(t) \leq p_{s,max}^T, \forall m \in \mathcal{M},$$

$$C2 : p_{w,min}^T \leq p_{w,n}^T(t) \leq p_{w,max}^T, \forall n \in \mathcal{N}, \quad (11)$$

$$C3 : \sum_{m=0}^M k_{s,m}(t) \leq 1, \forall m \in \mathcal{M},$$

$$C4 : \sum_{n=0}^N k_{w,n}(t) \leq 1, \forall n \in \mathcal{N}.$$

where constraints $C1$ and $C2$ restrict the transmission power of each SL-U user pair and Wi-Fi user, respectively. Constraints $C3$ indicates that only one SL-U user pair occupies the channel per slot at most. Constraint $C4$ shows that at most one Wi-Fi user occupies the channel per slot.

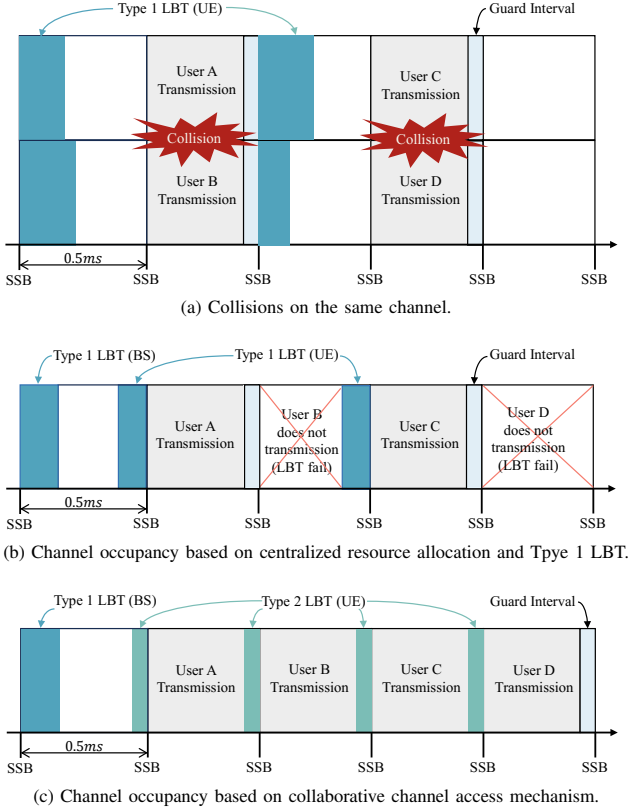


Fig. 3. Channel occupancy due to different schemes.

III. COLLABORATIVE CHANNEL ACCESS (CCHA)

In this section, we present a comprehensive explanation of the collaborative channel access mechanism. Furthermore, we describe the information acquisition process that supports these collaborative operations.

The 3GPP standard mandates that the minimum resource allocation unit for the PSSCH in the time domain is a slot. As a result, SL-U users operating in the unlicensed spectrum cannot immediately begin transmission after completing the LBT process; instead, they must wait until the next SSB to transmit data. This limitation significantly impacts the performance of SL-U systems. In a distributed resource allocation scheme, namely Mode 2, each SL-U user independently performs the LBT process and waits for the next SSB to transmit. However, this approach often results in frequent and severe collisions, as illustrated in Fig. 3(a). On the other hand, if SL-U users adopt a centralized resource allocation scheme, the collision issue can be mitigated. Nevertheless, if only Type 1 LBT is employed, the LBT process may fail due to the channel occupied in the previous slot by other SL-U users, resulting in low channel resource utilization, as shown in Fig. 3(b). To overcome these challenges, we propose a collaborative channel access mechanism that optimizes resource utilization and improves the overall performance of SL-U systems.

The mechanism integrates multiple LBT types with a centralized resource allocation strategy to enhance efficiency and coordination. First, the BS performs the Type 1 LBT process to compete for channel access. Upon successful completion, the BS obtains the channel's time-domain occupancy period,

denoted as T_{cot} , and the channel bandwidth B in the frequency domain. The BS then centrally allocates these resources, dividing them into slots for SL-U users with data to transmit within its coverage area. SL-U users assigned specific channel resources validate their availability by performing the Type 2 LBT process at a designated position before the SSB. If the Type 2 LBT process is completed, the user proceeds with data transmission, as illustrated in Fig. 3(c).

For LBT channel access, this study specifies that all channel sensing processes must begin at the SSB for experimental convenience, except for specific channel sensing positions designated by the base station. While implementing the collaborative channel access mechanism proposed in this study, the base station and SL-U users exchange control signals to facilitate collaborative operations. To ensure the reliability of control signaling transmission, these signals are conveyed over the licensed spectrum. Furthermore, by the standard, SL-U users avoid transmitting data during the final orthogonal frequency division multiplexing (OFDM) symbol of the allocated resources to establish a guard interval (GI).

IV. JOINT OPTIMIZATION OF CHANNEL ACCESS AND POWER CONTROL BASED ON C-GHDRL

In this section, we first elaborate on the fundamental concepts of semi-Markov decision processes and hierarchical reinforcement learning. Subsequently, we introduce the C-GHDRL algorithm, designed to achieve the joint optimization of channel access and power control.

A. SMDP and Hierarchical Reinforcement Learning

The Markov Decision Process (MDP) is commonly employed to model scenarios in reinforcement learning (RL), primarily addressing traditional decision-making processes. However, in real-world scenarios, the intervals between decision-making stages can be variable, which poses challenges for standard MDPs in accurately modeling such problems. The Semi-Markov Decision Process (SMDP), as an extension of the MDP framework, offers an option-based decision-making model capable of addressing control problems characterized by variable decision times [38].

The Semi-Markov Decision Process is primarily defined by a five-tuple $\langle \mathcal{S}, \mathcal{A}, \mathcal{O}, \mathcal{P}, \mathcal{R} \rangle$, where \mathcal{O} denotes the set of options, and the remaining elements have meanings analogous to those in the standard MDP [39]. An option is represented as a triplet $\langle \mathcal{I}, \pi, \beta \rangle$, where $\mathcal{I} \subseteq \mathcal{S}$ indicates the set of initial states for the option, $\pi : \mathcal{S} \times \mathcal{A} \rightarrow [0, 1]$ represents the policy function associated with the option, and $\beta : \mathcal{S} \rightarrow [0, 1]$ denotes the probability of the option terminating in a given state. An option $\langle \mathcal{I}, \pi, \beta \rangle$ is available in state s_t if and only if $s_t \in \mathcal{I}$. Once the option is selected, actions are determined according to π until the option terminates stochastically based on β . Specifically, the execution of the Markov option proceeds as follows. First, the agent selects the next action a_t according to the probability distribution $\pi(s_t, \cdot)$. The environment then transitions to state s_{t+1} , where the option may terminate with probability $\beta(s_{t+1})$. If the option does not terminate, the agent determines the action a_{t+1} based on $\pi(s_{t+1}, \cdot)$ and possibly terminates in s_{t+2} according to $\beta(s_{t+2})$, and so on. Upon termination of the option, the agent can choose another option.

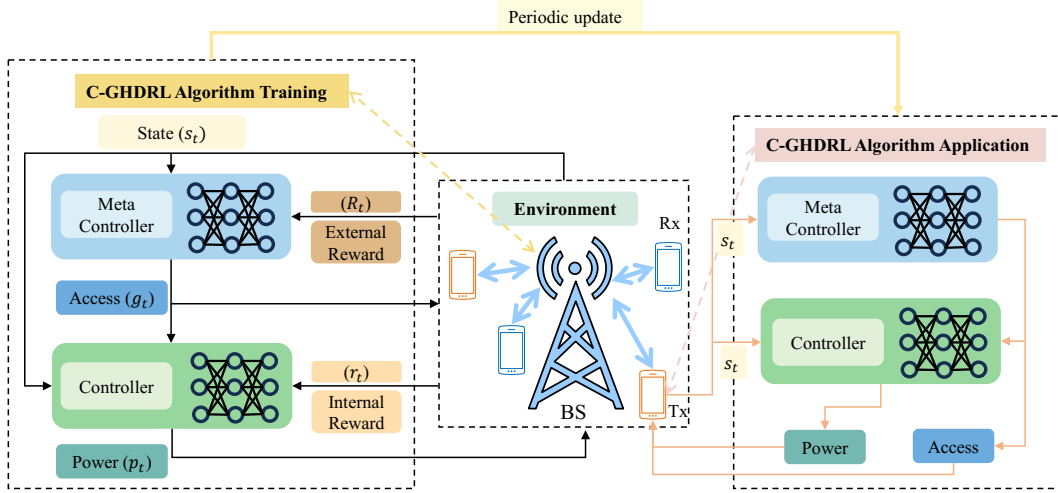


Fig. 4. Framework of the C-GHDRL algorithm.

Hierarchical Reinforcement Learning (HRL) is a significant subfield of reinforcement learning that distinguishes itself from classic RL by being grounded in the SMDP framework. HRL enhances the traditional RL approach through hierarchical abstraction, addressing challenges like sparse rewards, sequential decision-making, and limited transferability, which are often difficult to resolve in conventional RL. By structuring decision processes hierarchically, HRL promotes more effective exploration and improved transfer learning capabilities. Despite these advantages, HRL still faces limitations in computational power and inefficiency in expressing complex state features, particularly in continuous state-action spaces. With the advent of DRL, HDRL emerged by integrating deep learning (DL) techniques into the HRL framework. This integration not only expands the theoretical foundation of HRL but also leverages deep neural networks to enhance feature extraction and policy learning. Consequently, HDRL exhibits a more efficient and flexible hierarchical structure, making it well-suited for solving complex tasks that were previously intractable using standard HRL methods.

Subgoal-based Hierarchical Deep Reinforcement Learning (GHDL) differs from traditional HRL by not explicitly defining options. Instead, it identifies specific states as subgoals, represented by the set \mathcal{G} . The process of moving from the current state s to a subgoal $g \in \mathcal{G}$ is treated as an option, and an upper-level policy $\pi_h : \mathcal{S} \rightarrow \mathcal{G}$ is learned based on the external reward \mathcal{R}^{out} . This approach incrementally guides the agent toward completing the overall task. The design of subgoals effectively constructs multiple SMDPs, breaking down the original problem into smaller, more manageable tasks and reducing the complexity of the state space. Transitioning between sub-goals signifies the completion of a specific sub-task, providing a crucial mechanism for addressing sequential decision-making processes [40].

Universal Value Function Approximators (UVFA) form the theoretical basis for the GHDL framework, allowing most classic DRL algorithms to be seamlessly integrated as the underlying algorithms of GHDL. In this framework, the

upper-layer controller takes the current state s as input and outputs a sub-goal g . The lower-layer controller then uses the state-subgoal pair (s, g) as an extended state to learn the lower-layer policy π . The upper-layer policy is trained based on external rewards, while the lower-layer policy is optimized using internal rewards [33]. For any extended state (s, g) and internal reward r^{in} , the formula for the extended state value function $V_\pi(s, g)$ is defined as:

$$V_\pi(s, g) = \mathbb{E} \left[\sum_{t=0}^{\infty} r^{in}(s_t, a_t) \prod_{k=0}^t \gamma_g(s_k) \mid s_0 = s \right], \quad (12)$$

where γ_g represents the discount coefficient under the subgoal constraint.

Correspondingly, the formula for the extended state-action value function $Q_{pi}(s, g, a)$ is defined as:

$$Q_{pi}(s, g, a) = \mathbb{E}_{s'} [r^{in}(s, a) + \gamma_g(s') V_\pi(s', g)]. \quad (13)$$

B. Channel Access and Power Control based on C-GHDRL

The joint optimization of channel access and power control can be decomposed into two sub-problems: channel access and power control. This hierarchical structure with multi-step decomposition is particularly well-suited for the GHDL algorithm. However, in the unlicensed spectrum, because of the absence of an information-sharing mechanism among SL-U users, SL-U users are restricted to sense only their local environment. This restriction prevents SL-U users from obtaining complete global information, which hinders the GHDL algorithm model from making globally optimal decisions.

To address this challenge, we developed a C-GHDRL algorithm framework, as illustrated in Fig. 4. In the framework, the BS collects comprehensive global information through collaborative interactions with SL-U users. The BS utilizes this information to train the C-GHDRL model, which is periodically distributed to all SL-U users to ensure continuous refinement and improvement in their decision-making accuracy. To reduce signaling overhead and latency, each SL-U user independently determines its channel access and transmission

power. When an SL-U user has data to transmit, the sensed channel state information is input into the user's local model to determine channel access and transmission power decisions.

In the framework, the C-GHDRL algorithm comprises two components: a meta-controller and a controller. The meta-controller is responsible for optimizing channel access, while the controller focuses on power control, utilizing the state information and outputs provided by the meta-controller. Since the state transition probabilities are unknown, we employ a deep Q-learning algorithm to train the policies of both the meta-controller and the controller within the C-GHDRL frame [41]. Specifically, the controller estimates the state-value function $Q_1(s, a; g)$ as follows:

$$\begin{aligned} Q_1(s, a; g) &= \max_{\pi_{ag}} \mathbb{E} \left[\sum_{t'=t}^{\infty} \gamma^{t'-t} r_{t'} \mid s_t = s, a_t = a, g_t = g, \pi_{ag} \right] \\ &= \max_{\pi_{ag}} \mathbb{E} [r_t + \gamma \max_{a_{t+1}} Q_1(s_{t+1}, a_{t+1}; g) \mid s_t = s, \\ &\quad a_t = a, g_t = g, \pi_{ag}], \end{aligned} \quad (14)$$

where g represents the goal of agent in state s and $\pi_{ag} = \mathcal{P}(a|s, g)$ is the action policy. r_t represents the internal reward provided to the controller.

Similarly, for the meta controller, the state-value function $Q_2(s, g)$ is defined as:

$$\begin{aligned} Q_2(s, g) &= \max_{\pi_g} \mathbb{E} \left[\sum_{t'=t}^{t+N} R_t + \gamma \max_{g'} Q_2(s_{t+N}, g') \mid s_t = s, g_t = g, \pi_g \right], \end{aligned} \quad (15)$$

where N represents the number of time steps between two sub-goals. g' represents the goal of the agent in state s_{t+N} , and $\pi_g = \mathcal{P}(g|s)$ represents the policy over goals. R_t is reward signals received from the environment. It is worth noting that the transitions (s_t, g_t, R_t, s_{t+N}) generated by Q_2 operates at a slower time scale than the transitions $(s_t, a_t, g_t, r_t, s_{t+1})$ generated by Q_1 .

We represent $Q(s, g) \approx Q(s, g; \theta)$ using a nonlinear function approximator with parameters θ , known as a deep Q-network. Each $Q \in \{Q_1, Q_2\}$ can be trained by minimizing the corresponding loss functions, $L_1(\theta_1)$ and $L_2(\theta_2)$. The loss function for Q_1 can be expressed as:

$$L_1(\theta_1, i) = \mathbb{E}_{(s, a, g, r, s') \sim \mathcal{D}_1} [(y_{1,i} - Q_1(s, a; \theta_{1,i}, g))^2], \quad (16)$$

where i denotes the training iteration number and $y_{1,i} = r + \gamma \max_{a'} Q_1(s', a'; \theta_{1,i-1}, g)$.

When optimizing the loss function, the parameter $\theta_{1,i-1}$ from the previous iteration remains unchanged. The parameter θ_1 can be optimized using the gradient:

$$\begin{aligned} \nabla_{\theta_{1,i}} L_1(\theta_{1,i}) &= \mathbb{E}_{(s, a, r, s' \sim \mathcal{D}_1)} [(r + \gamma \max_{a'} Q_1(s', a'; \theta_{1,i-1}, g) - \\ &\quad Q_1(s, a; \theta_{1,i}, g)) \nabla_{\theta_{1,i}} Q_1(s, a; \theta_{1,i})], \end{aligned} \quad (17)$$

The loss function $L_2(\theta_2)$ and its gradients can be derived using a similar procedure.

Consequently, the C-GHDRL algorithm implemented in our framework is built upon the subgoal-based hierarchical deep

Algorithm 1 : Learning algorithm base on C-GHDQN

- 1: Initialize experience replay memories $\{\mathcal{D}_1, \mathcal{D}_2\}$ to capacity $\{\mathcal{C}_1, \mathcal{C}_2\}$ for the controller and meta-controller respectively
 - 2: Initialize $\{Q_1, Q_2\}$ network parameters with random weights $\{\theta_1, \theta_2\}$ for the controller and meta-controller respectively
 - 3: Initialize target $\{Q'_1, Q'_2\}$ network parameters with random weights $\{\theta'_1, \theta'_2\}$ for the controller and meta-controller respectively
 - 4: Initialize exploration probability $\varepsilon_{1,g} = 1$ for the controller for all goals g and $\varepsilon_2 = 1$ for the meta-controller.
 - 5: **for** $i = 1, num_episodes$ **do**
 - 6: Initialize communication system and get start state description s
 - 7: Obtain subgoal g through Q_2 network according to ε -greedy
 - 8: **while** s is **not** terminal **do**
 - 9: $R = 0$
 - 10: $s_0 \leftarrow s$
 - 11: **while not** (s is terminal **or** goal g reached) **do**
 - 12: Obtain a through Q_1 network according to ε -greedy
 - 13: Execute a and obtain next state s' and obtain intrinsic reward $r(s, a, s')$ from controller
 - 14: Store transition $(\{s, g\}, a, r, \{s', g\})$ in \mathcal{D}_1
 - 15: Randomly sample mini-batches from \mathcal{D}_1 and perform a gradient descent by $L_1(\theta_{1,i})$ with respect to the network parameters θ_1
 - 16: Every C steps copy current network weights into target network $\theta'_1 \leftarrow \theta_1$
 - 17: $R \leftarrow R + r$
 - 18: $s \leftarrow s'$
 - 19: **end while**
 - 20: Store transition (s_0, g, R, s') in \mathcal{D}_2
 - 21: Randomly sample mini-batches from \mathcal{D}_2 and perform a gradient descent by $L_2(\theta_{2,i})$ with respect to the network parameters θ_2
 - 22: Every C steps copy current network weights into target network $\theta'_2 \leftarrow \theta_2$
 - 23: **if** s is **not** terminal **then**
 - 24: Obtain g through Q_2 network according to ε -greedy
 - 25: **end if**
 - 26: **end while**
 - 27: **end for**
-

Q network (GHDQN) model. The fundamental parameters (agent, state, goal, action, reward) in the C-GHDQN algorithm proposed in this paper are as follows:

1) *Agent*: We propose a centralized optimization method employing BS as an agent. The BS utilizes data from all users to learn about global policy.

2) *Subgoal*: The subgoal space \mathcal{G} output by the upper layer meta controller is defined as follows: if the channel is to be accessed, $g(t) = 1$; otherwise, $g(t) = 0$.

3) *State*: For the upper layer meta controller, its state is

$$s_{mc}(t) = [p_s^T(t-1), \mathbf{p}_{ch}^R(t)], \quad (18)$$

where $p_s^T(t-1)$ represents the power sent by the SL-U user at the last slot, and $\mathbf{p}_{ch}^R(t)$ represents the channel energy detected by all SL-U users except itself. For the lower layer controller, it is an extended state represented as follows:

$$\begin{aligned} s_c(t) &= [s_{mc}(t), g(t)] \\ &= [p_s^T(t-1), \mathbf{p}_{ch}^R(t), g(t)], \end{aligned} \quad (19)$$

4) *Action*: The action space \mathcal{A} represents the power adjustment operation. At each slot t , the action $a_t \in \mathcal{A}$ can be defined as

$$\mathcal{A} = [p_{s,min}^T, \dots, p_{s,max}^T]. \quad (20)$$

5) *Reward*: In order to enhance the transmission rate of the coexistence system while maintaining fairness, we define the internal reward $r_t(g)$ and the external reward (environmental reward) R_t as:

$$r_t(g) = \begin{cases} U, & \eta_s \geq \eta_{s,min} \text{ and } \eta_w \geq \eta_{w,min} \\ -U, & \text{otherwise.} \end{cases} \quad (21)$$

$$R_t = \sum r_t(g). \quad (22)$$

We use a deep Q network (DQN) to learn optimal policies for the controller and meta controller. Algorithm 1 shows the specific steps of our C-GHDQN method.

V. SIMULATION RESULT

In this section, we first present the key parameters of the simulation scenario. Following that, we conduct a performance analysis of the CCHA mechanism. Finally, we evaluate the effectiveness of the C-GHDRL algorithm in addressing the joint optimization of channel access and power control.

A. Simulation Settings

We simulate a coexistence scenario in which SL-U and Wi-Fi users operate within a $400 \times 400 m^2$ indoor environment. In this simulation, a transmission from either SL-U or Wi-Fi users is considered successful when the conditions $\eta_{s,m} \geq \eta_{s,min}$ and $\eta_{w,n} \geq \eta_{w,min}$ are met. The traffic model for users in the coexistence system follows FTP Model 3 [41]. For clarity and convenience, the detailed simulation parameters are summarized in Table II.

In our experiments, the deep neural network (DNN) used to approximate the action-value function is composed of three fully connected feedforward hidden layers. The number of neurons in the three hidden layers is 256, 256, and 512, respectively. The Rectified Linear Unit (ReLU) activation function is applied to the first and second hidden layers, and the tanh activation function is used for the third layer. The experience replay memory \mathcal{D} has a capacity \mathcal{C} of 1000, and the Adam optimizer is employed to update the network weights θ , with a minibatch size of 256. The exploration probability ϵ decreases linearly from 1 to 0 throughout the iterations. The discount factor γ is set to 0.8, and the learning rate is 10^{-3} .

B. Performance of the CCHA mechanism

TABLE II
SIMULATION PARAMETERS

Parameters	Value
number of SL-U user pairs (M)	[20, 24, 28, 32]
number of Wi-Fi users (N)	[20, 24, 28, 44]
distance between Rx and Tx of SL-U (dis_{random})	[1m, 5m]
carrier center frequency (f_c)	5.8 GHz
channel bandwidth (B)	20 MHz
sub-carrier space	30 KHz
channel occupancy time (T_{cot})	2 ms
power spectral density of AWGN	-174 dBm/Hz
SIFS	16 μs
DIFS	34 μs
T_d	34 μs
T_{sl}	9 μs
weighted factor(β)	0.8
period of traffic	10 ms
user's model update time	100 ms
transport block size	300 Bytes
$\eta_{s,min}$	15 dB
$\eta_{w,min}$	6 dB

To evaluate the effectiveness of our proposed CCHA mechanism, we analyze the experimental results from four comparative schemes. In these simulations, we set the transmission power for both SL-U users and Wi-Fi users at 23 dBm. Furthermore, we established a lower channel sensing threshold to reduce the possibility of resource reuse between SL-U users and Wi-Fi users, thereby highlighting the advantages of the CCHA mechanism.

- 1) **CCHA**: The CCHA mechanism integrates channel access and resource allocation. The specific details are described in Section IV.
- 2) **CCHA-T1**: The only difference between the scheme and the scheme of CCHA is in the channel access mechanism for SL-U users. In the scheme, when SL-U users want to send data, they need to perform Type 1 LBT.
- 3) **T12-LBT and DRA**: Unlike the CCHA scheme, in the scheme, resources are independently acquired by each SL-U user, which is referred to as distributed resource allocation (DRA). Additionally, when an SL-U user needs to transmit data, the user first performs Type 1 LBT. Upon successful completion, Type 2 LBT is performed at the designated position before the next SSB.
- 4) **T10-LBT and DRA**: The only difference between this scheme and the scheme of T12-LBT and DRA is that SL-U users do not need to perform a Type 2 LBT before SSB.

We compare the differences between the scheme proposed in this paper and other schemes in terms of Jain's fairness index, packet reception rate (PRR), throughput, and waiting time. PRR is the ratio of the number of successfully received packets to the total number of packets sent. The waiting time is the duration from the generation to the successful transmission of a transport block. Throughput, denoted by Th , is defined as the rate of network transmission per unit of time, with the

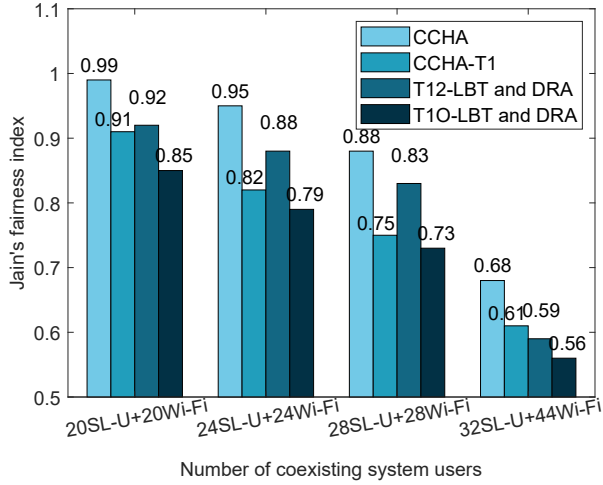


Fig. 5. Comparisons of Jain's fairness index over difference schemes.

unit expressed in bits per second (bps).

$$Th = \frac{P_{success} \times TB_{size}}{Time}, \quad (23)$$

where $P_{success}$ is the number of successfully received packets by SL-U. The TB_{size} is the transport block size. $Time$ is simulation time.

Fig. 5 illustrates the comparison of Jain's fairness index across the four schemes as the number of system users increases. First, it can be seen from the figure that as the number of users increases, the Jain's fairness index of all schemes decreases. The decrease is caused by system resources becoming increasingly scarce as the number of users increases. Then, we observed that the scheme utilizing the CCHA is superior to other comparative schemes regarding Jain's fairness index. The reasons include two aspects. On the one hand, the advantages of the two types of channel access are fully utilized in the CCHA mechanism. Type 1 LBT performed by the base station can sense whether the channel is idle initially, while Type 2 LBT performed by the SL-U user can sense whether the channel is idle again before SSB, with a shorter sensing time compared to Type 1 LBT. Therefore, the mechanism effectively ensures fairness while enhancing resource utilization. On the other hand, centralized resource allocation (CRA) is used in the CCH, which can ensure that the resources in the SL-U system are completely orthogonal. This method effectively prevents collisions arising from multiple SL-U users selecting the same resources for data transmission due to the absence of a coordination mechanism in the DRA. In addition, the scheme of T10-LBT and DRA exhibits the poorest performance in terms of Jain's fairness index. This is because the T10-LBT scheme requires SL-U users to perform only Type 1 LBT without reconfirming whether the channel is idle before access. This limitation significantly increases the likelihood of collisions with users already occupying the channel. Furthermore, the absence of a coordination mechanism in the DRA scheme leads to increased potential for collisions among SL-U users, further degrading system performance.

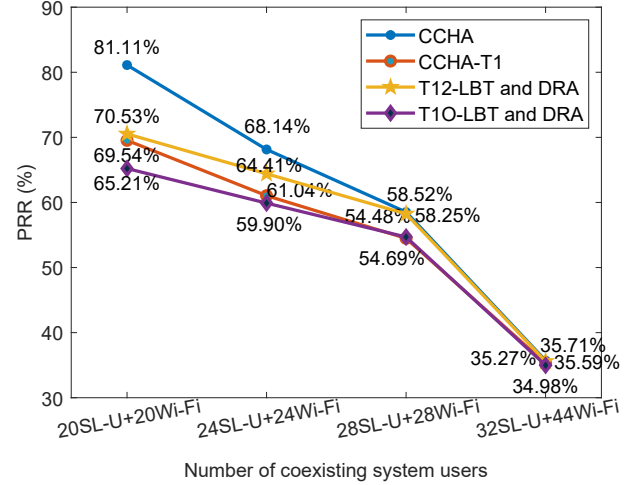


Fig. 6. Comparisons of PRR over difference schemes.

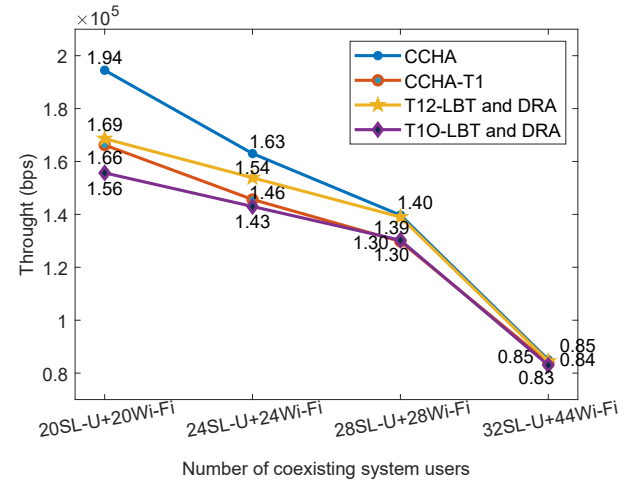


Fig. 7. Comparisons through over difference schemes.

Fig. 6 and Fig. 7 illustrate the PRR and throughput results for varying numbers of users in the system. The results indicate that PRR and throughput degrade as the number of users increases. This performance decline is attributed to the increasing scarcity of resources as the user density rises. Furthermore, if the number of users increases to a certain scale, the performance deteriorates sharply due to severe resource contention. Notably, under moderate user density, the CCHA scheme outperforms others regarding PRR and throughput. This improvement is due to the CCHA scheme's ability to effectively mitigate the conflict inherent in distributed resource allocation methods while enhancing channel access opportunities for SL-U users in the unlicensed spectrum.

Fig. 8 presents the waiting time for SL-U and Wi-Fi users under different channel access mechanisms and varying numbers of system users. Since the channel access mechanism is the primary factor influencing waiting time, we focus on comparing the waiting time across different channel access types with centralized resource allocation. First, as the number of users increases, we can observe that the waiting time also increases. The reason is that increased competition for access

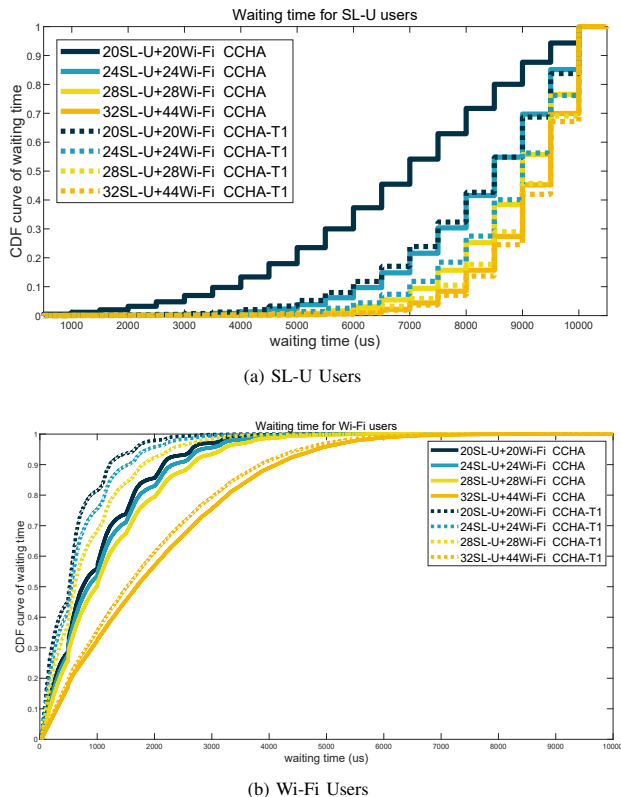


Fig. 8. Comparisons waiting time between CCHA and CCHA-T1.

channels intensifies channel contention, leading to longer delays. The waiting time under the CCHA scheme is shorter than that under the CCHA-T1 scheme, as in Fig. 8(a). This difference arises because, in the CCHA mechanism, SL-U users perform Type 2 LBT before the SSB. This allows the channel status to be determined in a shorter sensing period, enabling SL-U users to access the channel more quickly than those performing Type 1 LBT under the CCHA-T1 scheme. Conversely, as shown in Fig. 8(b), the waiting time for Wi-Fi users in a system employing the CCHA mechanism is slightly longer than that for Wi-Fi users in a system using the CCHA-T1 mechanism, which indicates that, while the CCHA mechanism enhances access opportunities for SL-U users, it introduces a certain degree of impact on Wi-Fi users. However, this impact remains acceptable, ensuring effective coexistence between SL-U and Wi-Fi users. Furthermore, as the number of users increases beyond a certain scale, the waiting times for users under both schemes are relatively close, indicating that the CCHA scheme is not suitable for scenarios involving large-scale user deployments.

C. Performance of the Proposed C-GHDRL

As the number of users increases, system performance degrades significantly due to resource constraints. To address this, SL-U and Wi-Fi users are allowed to perform appropriate resource reuse, improving the overall performance of the coexistence system. To achieve this, we employ the C-GHDRL algorithm to jointly optimize the channel access and transmission power for SL-U users, further enhancing system performance. In this section, the numbers of SL-U and Wi-

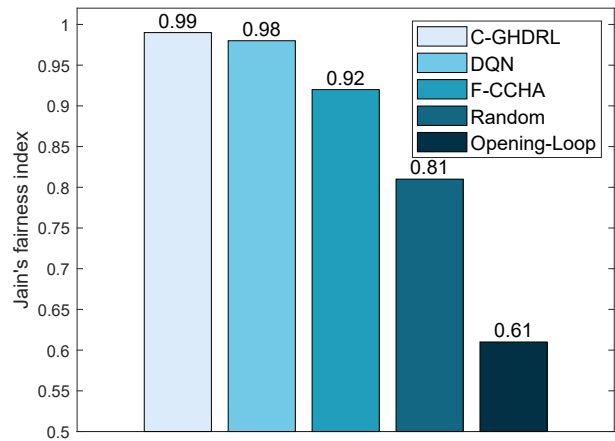


Fig. 9. Comparisons the Jain's fairness index over difference schemes.

Fi users are set to 32 and 44, respectively. Additionally, the transmission power of SL-U users is set between -40 dBm and 0 dBm due to the relatively short distance between their transmitters and receivers. Meanwhile, Wi-Fi users dynamically adjust their transmission power using a closed-loop power control strategy to adapt to the dynamic variations in the channel environment.

To verify the performance of the C-GHDRL algorithm, we utilize four schemes for comparison, i.e., the DQN algorithm, random algorithm, open-loop power control algorithm, and the fundamental scheme of CCHA (F-CCHA).

- 1) **C-GHDRL algorithm:** The C-GHDRL algorithm-based scheme builds upon the F-CCHA scheme and leverages the C-GHDRL algorithm to dynamically adjust channel access and transmission power for SL-U users. For further details, refer to Section V.
- 2) **DQN algorithm:** The DQN algorithm-based scheme builds upon the F-CCHA scheme and leverages the DQN algorithm to dynamically adjust transmission power for SL-U users.
- 3) **Random algorithm:** The random algorithm-based scheme builds upon the F-CCHA scheme and leverages the random algorithm to dynamically adjust channel access and transmission power for SL-U users.
- 4) **Open-loop power control algorithm:** The open-loop power control algorithm-based scheme builds upon the F-CCHA scheme and leverages the open-loop power control algorithm to dynamically adjust transmission power for SL-U users.
- 5) **F-CCHA:** The F-CCHA scheme acts as a benchmark scheme that employs the CCHA mechanism for SL-U users. In the scheme, the LBT energy sensing threshold for SL-U users is fixed, and their transmission power is 0 dBm.

Fig. 9 shows the comparison of Jain's fairness index of five different schemes. As can be seen from the figure, Jain's fairness index of the schemes based on the C-GHDRL and the DQN algorithm is higher than the benchmark scheme of F-CCHA. The phenomenon shows that schemes based on the C-GHDRL and DQN algorithms can improve the performance

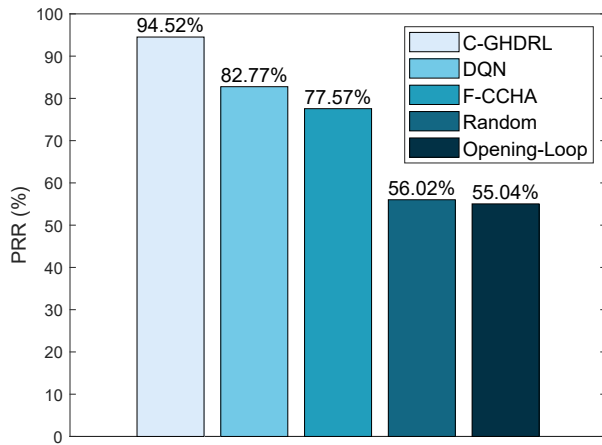


Fig. 10. Comparisons the PRR over difference schemes.

of coexistence systems. However, the scheme based on the DQN algorithm improves system performance less than the scheme based on the C-GHDRL algorithm. This is because the scheme based on the C-GHDRL algorithm effectively ensures the coexistence of SL-U users and Wi-Fi users by adjusting the transmission power and channel access opportunities of SL-U users, thereby achieving the highest Jain's fairness index. The scheme based on the DQN algorithm cannot control channel access opportunities, which has a certain impact on Wi-Fi users, resulting in a slight decrease in Jain's fairness index. Furthermore, Jain's fairness index of the random scheme and the open-loop power control-based scheme is lower than the benchmark scheme of F-CCHA. This is because the random scheme is unpredictable regarding transmission power and channel access opportunities. Therefore, the impact on Wi-Fi users cannot be controlled, resulting in a low Jain's fairness index. Based on the open-loop power control scheme, SL-U users cannot detect interference in the channel, which seriously affects the performance of the coexistence system and makes Jain's fairness index of this scheme the smallest.

Fig. 10 shows the PRR performance of five different schemes. As depicted in the figure, the PRR of the scheme utilizing the C-GHDRL and the DQN algorithm is higher than the benchmark scheme of F-CCHA. Notably, the scheme employing the C-GHDRL algorithm exhibits the highest PRR. This is because adjusting the transmission power and channel access opportunities of SL-U users can effectively increase the transmission success rate of both SL-U users and Wi-Fi users. In addition, since the scheme based on the DQN algorithm only adjusts the transmission power of SL-U users, its PRR is lower than the scheme based on the C-GHDRL algorithm. From the figure, we can also observe that both the random scheme and the scheme based on open-loop power control have lower PRR than the benchmark scheme of F-CCHA. This is because the two schemes have shortages in adjusting the transmission power and channel access opportunities of SL-U users. The random scheme involves randomness in both transmission power and access channel. Although the scheme of open-loop power control can determine the transmission power by calculating the path loss based on the reference

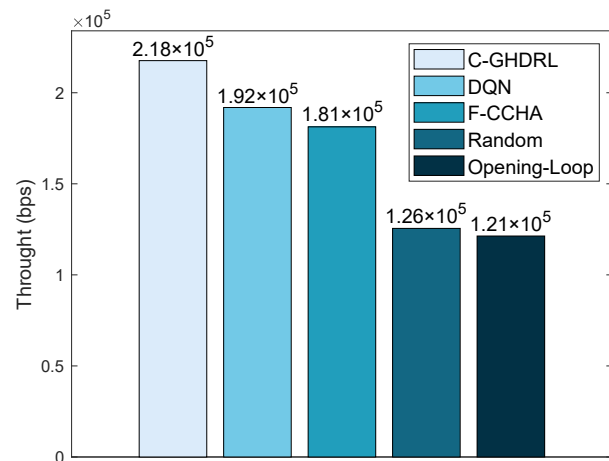


Fig. 11. Comparisons the throughut over difference schemes.

signal, it cannot estimate the interference power in the channel. Therefore, it is difficult for the power adjustment strategy in the open-loop power control scheme to calculate a transmission power that guarantees successful data transmission for SL-U users.

Fig. 11 shows the throughput performance of various schemes. The reasons and phenomena are the same as PRR in Fig. 10.

VI. CONCLUSION

In this paper, we investigate methods to enhance the overall performance of coexistence systems operating in the unlicensed spectrum while ensuring fair coexistence between SL-U users and Wi-Fi users. First, we propose a CCHA mechanism that integrates channel access with resource allocation. This mechanism enhances spectrum fairness in coexistence systems while improving spectrum utilization. Next, we formulate a joint mathematical model for channel access and power control, aiming to achieve a balance between fairness and transmission rate. Finally, we develop a C-GHDRL algorithm framework. The framework enables joint optimization of channel access and power control through collaborative interactions between the BS and SL-U users, thereby significantly enhancing the overall performance of the coexistence system. Future research will focus on exploring more efficient collaborative mechanisms under conditions of incomplete global information.

REFERENCES

- [1] M. Khan, A. Haleem, and M. Javaid, "Changes and improvements in Industry 5.0: A strategic approach to overcome the challenges of Industry 4.0," *Green Technologies and Sustainability*, vol. 1, no. 2, pp. 2949–7361, 2023.
- [2] H. R. Chi, C. K. Wu, N.-F. Huang, K.-F. Tsang, and A. Radwan, "A Survey of Network Automation for Industrial Internet-of-Things Toward Industry 5.0," *IEEE Transactions on Industrial Informatics*, vol. 19, no. 2, pp. 2065–2077, 2023.
- [3] Z. Zhang and S. Wang, "Visible Thermal Person Reidentification via Mutual Learning Convolutional Neural Network in 6G-Enabled Visual Internet of Things," *IEEE Internet of Things Journal*, vol. 8, no. 20, pp. 15 259–15 266, 2021.
- [4] OPPO, "New WID on NR sidelink evolution (RP-213678)," *3rd Generation Partnership Project (3GPP)*, vol. 6, Dec. 2021.

- [5] V. Rajendran, G. Prasad, L. Lampe, and G. Vos, "SCUBA: An In-Device Multiplexed Protocol for Sidelink Communication on Unlicensed Bands," *IEEE Internet of Things Journal*, vol. 8, no. 22, pp. 16637–16652, 2021.
- [6] Y. Gao, Z. Zhang, H. Hu, X. Wang, Y. Jin, and X. Chu, "Fair and Efficiency Coexistence Between NR-U and WiGig Networks Enabled by a Matching-Based Framework With Forbidden Pairs," *IEEE Transactions on Vehicular Technology*, vol. 72, no. 9, pp. 11814–11827, 2023.
- [7] R. K. Saha, "Coexistence of Cellular and IEEE 802.11 Technologies in Unlicensed Spectrum Bands -A Survey," *IEEE Open Journal of the Communications Society*, vol. 2, pp. 1996–2028, 2021.
- [8] F. Slimeni, N. Fezai, Z. Chtourou, and A. B. Amor, "Optimal Power Allocation Based Unlicensed Spectrum Sharing for Cellular Networks," in *2022 5th International Conference on Advanced Systems and Emergent Technologies (IC_ASET)*, 2022, pp. 178–182.
- [9] 3GPP, "Physical layer procedures for shared spectrum channel access (Release 18)," 3rd Generation Partnership Project (3GPP), Technical Specification (TS) 37.213, Sep. 2024, v18.4.0.
- [10] 3GPP, "Physical layer procedures for data (Release 18)," 3rd Generation Partnership Project (3GPP), Technical Specification (TS) 38.214, Sep. 2024, v18.4.0.
- [11] V. Weerackody, H. Yin, and S. Roy, "NR Sidelink Mode 2 in Unlicensed Bands: Throughput Model & Validation," *IEEE Transactions on Communications*, pp. 1–1, 2024.
- [12] V. Loginov, E. Khorov, A. Lyakhov, and I. F. Akyildiz, "CR-LBT: Listen-Before-Talk With Collision Resolution for 5G NR-U Networks," *IEEE Transactions on Mobile Computing*, vol. 21, no. 9, pp. 3138–3149, 2022.
- [13] X. Xu, Q. Chen, H. Jiang, and J. Huang, "Millimeter-Wave NR-U and WiGig Coexistence: Joint User Grouping, Beam Coordination, and Power Control," *IEEE Transactions on Wireless Communications*, vol. 21, no. 4, pp. 2352–2367, 2022.
- [14] L. Wang, Z. Fei, M. Zeng, B. Li, Y. Huo, X. Dong, and Q. Cui, "Spatial-Reuse-Based Efficient Coexistence for Cellular and WiFi Systems in the Unlicensed Band," *IEEE Internet of Things Journal*, vol. 9, no. 3, pp. 1885–1898, 2022.
- [15] G. G. Girmay, Q.-V. Pham, and W.-J. Hwang, "Joint channel and Power Allocation for Device-to-Device Communication on Licensed and Unlicensed Band," *IEEE Access*, vol. 7, pp. 22196–22205, 2019.
- [16] A. S. Matar and X. Shen, "Joint Optimization of User Association, Power Control, and Dynamic Spectrum Sharing for Integrated Aerial-Terrestrial Network," *IEEE Journal on Selected Areas in Communications*, vol. 43, no. 1, pp. 396–409, 2025.
- [17] Y. Su, L. Huang, and M. LiWang, "Joint Power Control and Time Allocation for UAV-Assisted IoV Networks Over Licensed and Unlicensed Spectrum," *IEEE Internet of Things Journal*, vol. 11, no. 1, pp. 1522–1533, 2024.
- [18] K. Ganesan, "5G Advanced: Sidelink Evolution," *IEEE Communications Standards Magazine*, vol. 7, no. 1, pp. 58–63, 2023.
- [19] A. S. Matar and X. Shen, "Joint Subchannel Allocation and Power Control in Licensed and Unlicensed Spectrum for Multi-Cell UAV-Cellular Network," *IEEE Journal on Selected Areas in Communications*, vol. 39, no. 11, pp. 3542–3554, 2021.
- [20] H. Bao, Y. Huo, X. Dong, and C. Huang, "Joint Time and Power Allocation for 5G NR Unlicensed Systems," *IEEE Transactions on Wireless Communications*, vol. 20, no. 9, pp. 6195–6209, 2021.
- [21] C. Kai, H. Li, L. Xu, Y. Li, and T. Jiang, "Joint Subcarrier Assignment With Power Allocation for Sum Rate Maximization of D2D Communications in Wireless Cellular Networks," *IEEE Transactions on Vehicular Technology*, vol. 68, no. 5, pp. 4748–4759, 2019.
- [22] S. Huang, B. Liang, and J. Li, "Distributed Interference and Delay Aware Design for D2D Communication in Large Wireless Networks With Adaptive Interference Estimation," *IEEE Transactions on Wireless Communications*, vol. 16, no. 6, pp. 3924–3939, 2017.
- [23] Z. Zhou, B. Wang, B. Gu, B. Ai, S. Mumtaz, J. Rodriguez, and M. Guizani, "Time-Dependent Pricing for Bandwidth Slicing Under Information Asymmetry and Price Discrimination," *IEEE Transactions on Communications*, vol. 68, no. 11, pp. 6975–6989, 2020.
- [24] I. Budhiraja, N. Kumar, and S. Tyagi, "Deep-Reinforcement-Learning-Based Proportional Fair Scheduling Control Scheme for Underlay D2D Communication," *IEEE Internet of Things Journal*, vol. 8, no. 5, pp. 3143–3156, 2021.
- [25] Y. Shi, L. Lian, Y. Shi, Z. Wang, Y. Zhou, L. Fu, L. Bai, J. Zhang, and W. Zhang, "Machine Learning for Large-Scale Optimization in 6G Wireless Networks," *IEEE Communications Surveys & Tutorials*, vol. 25, no. 4, pp. 2088–2132, 2023.
- [26] M. Agarwal and V. Aggarwal, "Reinforcement learning for joint optimization of multiple rewards," *Journal of Machine Learning Research*, vol. 24, no. 49, pp. 1–41, 2023.
- [27] J. Tan, Y.-C. Liang, L. Zhang, and G. Feng, "Deep Reinforcement Learning for Joint Channel Selection and Power Control in D2D Networks," *IEEE Transactions on Wireless Communications*, vol. 20, no. 2, pp. 1363–1378, 2021.
- [28] N. Khan and S. Coleri, "Event-Triggered Reinforcement Learning Based Joint Resource Allocation for Ultra-Reliable Low-Latency V2X Communications," *IEEE Transactions on Vehicular Technology*, vol. 73, no. 11, pp. 16991–17006, 2024.
- [29] Y. Geng, E. Liu, R. Wang, and Y. Liu, "Hierarchical Reinforcement Learning for Relay Selection and Power Optimization in Two-Hop Cooperative Relay Network," *IEEE Transactions on Communications*, vol. 70, no. 1, pp. 171–184, 2022.
- [30] Y. Wang, Y. Liang, and Z. Wang, "Hierarchical Reinforcement Learning-Based Joint Allocation of Jamming Task and Power for Countering Networked Radar," *IEEE Transactions on Aerospace and Electronic Systems*, pp. 1–19, 2024.
- [31] H. Zhou, M. Elsayed, M. Bavand, R. Gaigalas, S. Furr, and M. Erol-Kantarci, "Cooperative Hierarchical Deep Reinforcement Learning Based Joint Sleep and Power Control in RIS-Aided Energy-Efficient RAN," *IEEE Transactions on Cognitive Communications and Networking*, pp. 1–1, 2024.
- [32] D. Kim, M. R. Castellanos, and R. W. Heath, "Joint Band Assignment and Beam Management Using Hierarchical Reinforcement Learning for Multi-Band Communication," *IEEE Transactions on Vehicular Technology*, vol. 73, no. 9, pp. 13451–13465, 2024.
- [33] Y. Huang and K.-W. Chin, "A Hierarchical Deep Learning Approach for Optimizing CCA Threshold and Transmit Power in Wi-Fi Networks," *IEEE Transactions on Cognitive Communications and Networking*, vol. 9, no. 5, pp. 1296–1307, 2023.
- [34] X. Li, Y. Zhang, H. Ding, and Y. Fang, "Intelligent Spectrum Sensing and Access With Partial Observation Based on Hierarchical Multi-Agent Deep Reinforcement Learning," *IEEE Transactions on Wireless Communications*, vol. 23, no. 4, pp. 3131–3145, 2024.
- [35] "IEEE Draft Standard for Information Technology - Telecommunications and Information Exchange Between Systems - Local and Metropolitan Area Networks - Specific Requirements - Part 11: Wireless LAN Medium Access Control (MAC) and Physical Layer (PHY) Specifications," *IEEE Draft P802.11-REVmb/D7.0, February 2011 (Revision of IEEE Std 802.11-2007, as amended by IEEE Std 802.11k-2008, IEEE Std 802.11r-2008, IEEE Std 802.11y-2008, IEEE Std 802.11w-2009 and IEEE Std 802.11n-2009)*, pp. 1–2198, 2011.
- [36] 3GPP, "Study on channel model for frequencies from 0.5 to 100 GHz (Release 17)," 3rd Generation Partnership Project (3GPP), Technical Report (TR) 38.901, Dec. 2023, v17.1.0.
- [37] H. Ko, J. Lee, and S. Pack, "A Fair Listen-Before-Talk Algorithm for Coexistence of LTE-U and WLAN," *IEEE Transactions on Vehicular Technology*, vol. 65, no. 12, pp. 10116–10120, 2016.
- [38] T. D. Kulkarni, K. Narasimhan, A. Saedi, and J. Tenenbaum, "Hierarchical deep reinforcement learning: Integrating temporal abstraction and intrinsic motivation," *Advances in neural information processing systems*, vol. 29, 2016.
- [39] Z. Qin, X. Zhang, X. Zhang, B. Lu, Z. Liu, and L. Guo, "The UAV trajectory optimization for data collection from time-constrained IoT devices: A hierarchical deep q-network approach," *Applied Sciences*, vol. 12, no. 5, p. 2546, 2022.
- [40] R. S. Sutton, D. Precup, and S. Singh, "Between MDPs and semi-MDPs: A framework for temporal abstraction in reinforcement learning," *Artificial intelligence*, vol. 112, no. 1-2, pp. 181–211, 1999.
- [41] 3GPP, "Study on Licensed-Assisted Access to Unlicensed Spectrum (Release 13)," 3rd Generation Partnership Project (3GPP), Technical Report (TR) 36.889, Jun. 2015, v13.0.0.